Original Article

Evaluation of structural skeletal asymmetry of the glenoid fossa in adult patients with unilateral posterior crossbite using surface-to-surface matching on CBCT images

Simone Muraglie[a]; Rosalia Leonardi[b]; Khaled Aboulazm[c]; Chiara Stumpo[a]; Carla Loreto[d]; Cristina Grippaudo[e]

ABSTRACT

Objectives: To compare, using surface-to-surface (StS) matching, any shape differences between the crossbite and noncrossbite side of the glenoid fossa and articular eminence in adult patients affected by posterior unilateral crossbite (PUXB) and compare them with unaffected controls.

Materials and Methods: 32 cone beam computed tomography (CBCT) scans of patients (mean age: 23.72 $\pm$ 3.74 years) undergoing surgical maxillary expansion were analyzed to obtain three-dimensional models of the left and right glenoid fossae that were superimposed using stable anatomical reference points and then compared using StS matching to evaluate the presence of any shape differences. These findings were compared with those obtained from 16 CBCT scans of unaffected controls (mean age: 23.72 $\pm$ 3.73 years).

Results: A mean difference of $>$11% was found between the study group and controls when comparing the matching percentages of the two sides of the glenoid fossa and articular eminence at all three levels of tolerance selected for this study. These differences were found to be highly statistically significant ($P \leq .0001$).

Conclusions: According to the shape analysis findings, adult PUXB patients exhibit a higher degree of glenoid fossa and articular eminence shape differences compared to unaffected controls. (*Angle Orthod.* 0000;00:000–000.)

KEY WORDS: Glenoid fossa; CBCT; Morphology; Articular eminence; Posterior crossbite

INTRODUCTION

Posterior crossbite (PXB) has been identified as a lingual inversion of the normal transverse relationship between the upper and lower dental arches, characterized by the buccal cusps of the maxillary teeth occluding lingually to the buccal cusps of the corresponding mandibular teeth.[1] PXB is one of the most frequently occurring malocclusions in the deciduous and mixed dentitions, with a reported prevalence of 7% to 23%[2–5] among malocclusions. The most common form of PXB is unilateral, with a functional shift of the mandible toward the crossbite side,[6] known as posterior unilateral crossbite (PUXB).

According to some authors,[6–10] if PUXB is left untreated during childhood it can lead to mandibular structural asymmetry. As far as temporomandibular joints (TMJ) are concerned, several studies[11–14] have identified or hypothesized positional asymmetry of the mandible in PUXB patients, postulating complex TMJ remodeling in response to asymmetric function and activity of the jaws and muscles in PUXB patients.[15]

However, most studies focused their attention mainly on the skeletal and positional asymmetries that occurred in mandibular bones (ie, mandibular condyles and ramus) and dental arches, while asymmetric TMJ

[a] Research Assistant, Department of Orthodontics, School of Dentistry, University of Catania, Catania, Italy.

[b] Full Professor, Department of Orthodontics, University of Catania, Catania, Italy.

[c] Assistant Professor, Department of Orthodontics, School of Dentistry, Pharos University, Alexandria, Egypt.

[d] Associate Professor. Department of Biomedical and Biotechnological Sciences, Human Anatomy and Histology Section, School of Medicine, University of Catania, Catania, Italy.

[e] Associate Professor, Department of Orthodontics, School of Dentistry, Universita Cattolica del Sacro Cuore, Rome, Italy.

Corresponding author: Dr Simone Muraglie, Department of Orthodontics, School of Dentistry, University of Catania, Policlinico Universitario "Gaspare Rodolico," Via S.Sofia, 78, 95123 Catania (CT), Italy
(e-mail: simonemuraglie@live.it)

Accepted: December 2019. Submitted: June 2019.
Published Online: February 3, 2020

glenoid fossa remodeling was not extensively evaluated.

Furthermore, the use of two-dimensional (2D) radiographic techniques and linear measurements for studying a three-dimensional (3D) structure, like the glenoid fossa and articular eminence, gave mixed results.

Recently, the introduction of cone beam computed tomography (CBCT) and 3D reconstruction of anatomical regions[16] have provided means for evaluation of the morphological features of many anatomical bony structures. Among these techniques, surface-to-surface matching (StS) is a superimposition and analysis technique that provides an accurate location of the shape mismatch zones. Accordingly, the aim of this study was to evaluate any morphological and shape differences between the crossbite and noncrossbite sides of the glenoid fossa and articular eminence in adult patients affected by PUXB and compare the findings with a control group by analyzing CBCT-derived 3D models through StS. The null hypothesis was that PUXB adult patients do not exhibit a greater degree of asymmetry between the crossbite and noncrossbite sides compared to a control group of unaffected subjects.

MATERIALS AND METHODS

A power analysis was carried out to evaluate the appropriate sample size for this research. The analysis indicated that 30 participants would yield a confidence level of 95% and a beta error level of 20%, and this would be adequate to determine statistically significant differences. The Institutional Review Board of the School of Dentistry, Catania University, approved the study.

For the study group (SG), 32 CBCT images (16 boys and 16 girls) were selected with a randomized block design to ensure the same number of subjects for each gender from a pool of 70 records of patients (45 boys and 25 girls) being treated with surgically assisted rapid maxillary expansion (SARME) referred (between January 2014 and November 2018) to a private dental practice. The pool of CBCT records was selected by inclusion and exclusion criteria. Inclusion criteria were presence of PUXB involving at least three posterior teeth in the malocclusion, Class I jaw relationship, full permanent dentition with the exception of the third molars, and history of mandibular shift during childhood. Exclusion criteria were presence of image artifacts, craniofacial deformities and/or severe facial asymmetry, history of previous orthodontic treatment and maxillofacial surgery, and history or clinical signs of TMJ disorders.

At the time of the scan, the mean age of the patients was 23.72 $\pm$ 3.73 years. The SG was age- and gender-matched with a control group (CG) of 16 CBCT images of patients (eight boys and eight girls, mean age: 24.31 $\pm$ 2.51 years) referred for third molar impaction or maxillary jaw cysts. The inclusion and exclusion criteria of the CG were the same as the SG except for the absence of the PUXB and the mandibular shift during childhood. All CBCT scans were taken with the NewTom 3G device (Quantitative Radiology, Verona, Italy), using a low-dose acquisition protocol[17] (110 kV, 6.19 mA, 0.25 mm voxel size, field of view: 12 inches) with the patient biting in maximum intercuspation and Frankfort horizontal plane parallel to the floor. All images were properly de-identified to protect patient confidentiality.

The images were assessed on a workstation using 300% magnification according to previously described protocols.[16,18–20] Two resident orthodontists (operators 1 and 2) were trained as examiners for glenoid fossa analysis using a set of CBCT scans (not included in this study).

Briefly, the CBCT scans were volume rendered using Mimics research software (version 19.0.0.347, Materialise NV, Leuven, Belgium) to obtain a 3D model of the glenoid fossa and articular eminence. Reverse engineering software (Geomagic Control X, version 2017.0.0, 3D Systems, Rock Hill, SC, USA) was used to achieve the StS analysis of the superimposed glenoid fossa and articular eminence models.

Workflow

Step 1. Generating the Segmentation Mask. The threshold sensitivity was set to "bone" and then adjusted scan by scan to detect the correct Hounsfield values for the entirety of the temporal bone and avoiding any over or under filling. The segmentation mask of the glenoid fossa was obtained from the surrounding craniofacial structures by manually cropping the sagittal and frontal views of the CBCT scans. The anteroposterior and craniocaudal boundaries of the region of interest (ROI) were defined by three points selected from the sagittal view (Figure 1A). First, the highest point of the glenoid fossa (UGF) was identified from the sagittal view and the corresponding slice was used as the reference sagittal CBCT slice. Then, two more points were selected:

- Articular eminence (AE): corresponding to the lowest point of the articular eminence.
- External auditory meatus (EAM): corresponding to the most anterior point on the external border of the external auditory meatus.

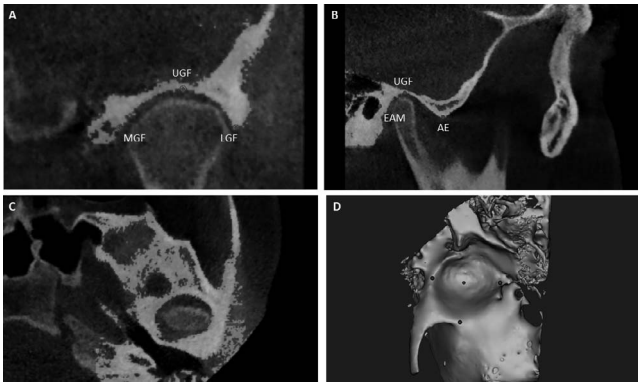

Figure 1. The segmentation mask was made by selecting three points in the sagittal view (A) and two points in the frontal view (B). (C) shows the axial image. The 3D model was rendered using Mimics software.

To identify the medial and lateral boundaries of the ROI, the reference slice of the frontal view was chosen as that passing though the UGF, previously identified from the sagittal view. Thus, two more points were selected (Figure 1B):

- Mesial glenoid fossa (MGF): the most medial point of the glenoid fossa.
- Lateral glenoid fossa (LGF): the most lateral point of the glenoid fossa.

Each side of the mask was extended by 30 mm.

Step 2. Generating the 3D model. The segmentation mask was rendered into a 3D glenoid fossa and articular eminence model (.stl) by using the specific function of the software (Figure 1D).

Step 3. Mirroring. Preliminary to the StS analysis, the 3D glenoid fossa model of the crossbite side (right side for the CG) was mirrored[19] by manually converting the image orientation from right-to-left to left-to-right (Figure 2A) to obtain the specular image of the crossbite side (or right side for CG).

Step 4. First registration. A point-based superimposition was made by selecting three points on the external surface of the original and mirrored 3D models (Figure 2B), chosen for high anatomical stability:

- The most anterior point on the external border of the external auditory meatus (aEAM).
- The most medial point of the foramen ovale of the sphenoid bone (FO).
- The most medial point of the foramen rotundum of the sphenoid bone (FR).

Step 5. Final registration, surface-based. The final registration was carried out using the "Best fit alignment" function, setting the unmirrored model as the reference data (Figure 2D).

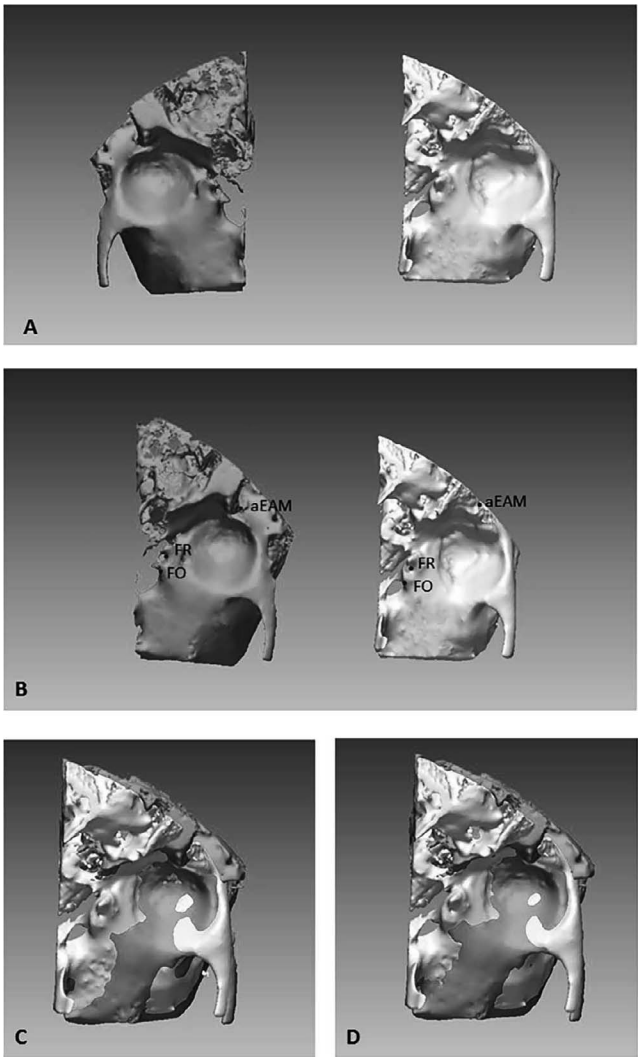

Figure 2. 3D model of the glenoid fossa mirrored on the X axis (A). The same three points were selected on mirrored and original models for the first registration (B, C). The final registration was made using the best fit algorithms (D).

Step 6. 3D deviation analysis. Once the specular models were finely overlapped, a 3D deviation analysis was performed using Geomagic Control X software. The linear distances (Euclidean distances) between 100% of the surface points of the two specular glenoid fossae models were calculated and represented on a 3D color map that showed the amount of deviation in different colors. Three tolerance levels were selected: (A) 0.50 mm; (B) 0.75 mm; and (C) 1.00 mm. The tolerance range values were graphically represented in green (Figure 3) while the values exceeding this range were shown in blue (for negative values) or red (for positive values). This analysis was designed to evaluate the inner surface of the glenoid fossae and articular eminence regions exclusively by selecting four more points (hemi-points) between the anatomical landmarks as shown in Figure 4.

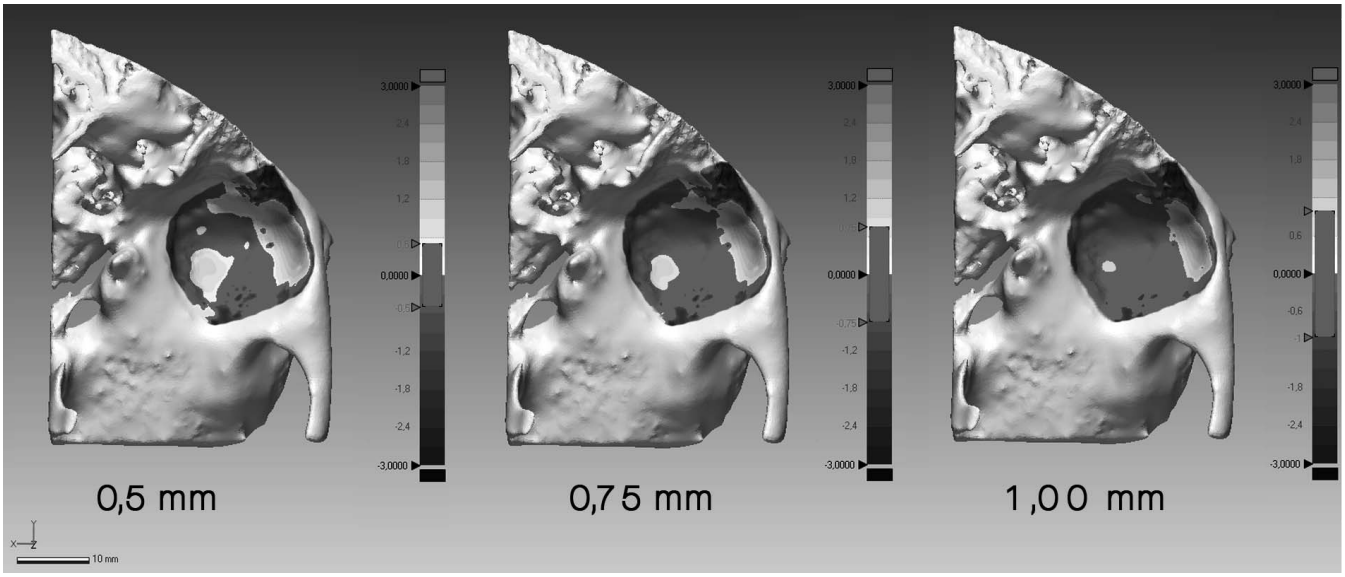

Figure 3. The surface-to-surface matching technique shows the deviation between the two glenoid fossa specular models previously superimposed. The values included in the tolerance range are graphically represented in green, while the ones exceeding this range are shown in blue (for negative values) or red (for positive values).

The maximum deviation calculation was set to ±3.00 mm. Once the deviation analysis was carried out, the percentages (%) of all the distance values within the tolerance range were calculated for the three tolerance groups.

Intraobserver reliability was evaluated by repeating the measurement process on 10 randomly selected CBCT images 4 weeks after the first examination by each operator who did not have access to their previous measurements.

Statistical Analysis

All the percentage measurements were recorded in a Microsoft Excel spreadsheet (Microsoft, Redmond, WA, USA) and analyzed using SPSS version 24 Statistics software (IBM Corporation, Armonk, New York, USA) and *P* values of less than .05 were considered statistically significant.

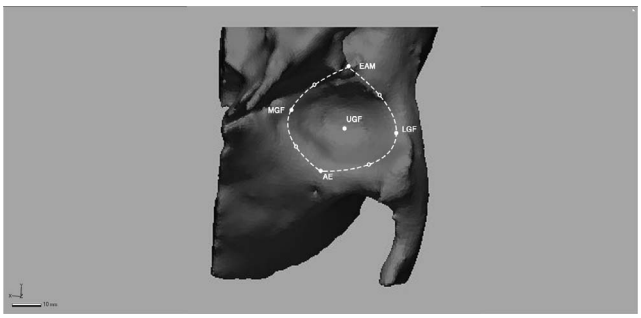

Figure 4. The glenoid fossa's inner surface for matching analysis was chosen by selecting the anatomical landmarks plus four more hemi-points.

To assess intraobserver and interobserver reliability, the threshold values (lower and higher) and landmark geometrical coordinates of the points obtained by each examiner for both measurement sets were statistically analyzed using the intraclass-correlation coefficient (ICC). Dahlberg's formula was used to assess the magnitude of random error.

The Kolmogorov–Smirnov test was used to test the normality of the data. As all the data was normally distributed with homogeneous variance, parametric tests were used to evaluate and compare the measurements.

A paired *t*-test was used to assess any differences in the matching percentages between the glenoid fossa and articular eminence regions of the crossbite and noncrossbite sides of SG and the right and left sides of CG.

RESULTS

Evaluating the intraobserver reliability, all the threshold values (lowest and higher value) were highly correlated with ICC values of 0.8332 and 0.9168 for operator 1 and 0.8228 and 0.8849 for operator 2. Evaluating the interobserver reliability, all the threshold values (lowest and higher) were highly correlated with ICC values of 0.8241 and 0.887. ICC values for geometrical coordinates of points selected were also highly correlated with ICC values ranging from 0.8456 and 0.8872 analyzing both intraobserver and interobserver reliability. The methodological error ranged from 0.40 to 0.58 percentage points.

Table 1. Comparison of the Differences Between Matching Percentage of Study and Control Groups for the Three Ranges of Tolerance Selected. Mean Percentage of Matching and its Standard Deviation (SD), Minimum and Maximum Values for Each Measurement. The Table Indicates the Values for Operator 1 and 2

	Operator 1																	
		Tolerance ±0.5 mm						Tolerance ±0.75 mm						Tolerance ±1.00 mm					
	Total	% Matching (Mean)	SD	Min.	Max.	Diff.	*P	% Matching (Mean)	SD	Min.	Max.	Diff.	*P	% Matching (Mean)	SD	Min.	Max.	Diff.	*P
Study group	32	60.01	2.38	55.43	65.98	12.60	.0001	71.78	1.26	69.45	74.55	11.61	.0001	80.55	1.46	78.09	84.08	11.17	.0001
Control group	16	72.55	2.74	68.90	77.34			83.39	1.59	81.03	86.88			91.73	1.70	89.34	95.87		
	Operator 2																	
		Tolerance ±0.5 mm						Tolerance ±0.75 mm						Tolerance ±1.00 mm					
	Total	% Matching (Mean)	SD	Min.	Max.	Diff.	*P	% Matching (Mean)	SD	Min.	Max.	Diff.	*P	% Matching (Mean)	SD	Min.	Max.	Diff.	*P
Study group	32	60.04	2.42	55.98	66.12	12.51	.0001	71.84	1.31	69.08	75.13	11.53	.0001	80.62	1.64	78.12	84.43	11.20	.0001
Control group	16	72.54	2.73	69.08	78.09			83.37	1.72	80.87	86.77			91.85	1.66	90.09	95.34		

* *P* value based on paired *t*-test.

The results for the matching percentages of the glenoid fossa and articular eminence regions between the crossbite and noncrossbite sides of PUXB patients and between the right and left sides of CG are given in Table 1.

Findings from the StS deviation analysis showed comparisons of the mean matching percentages between the glenoid fossa and articular eminence, and 3D models of patients and controls. For tolerance range A (0.50 mm), patients showed a mean matching percentage of 60.01% and controls showed a mean matching percentage of 72.55%. For tolerance range B (0.75 mm), patients showed a mean matching percentage of 71.78% and controls showed a mean matching percentage of 83.39%. For tolerance range C (1.00 mm), patients showed a mean matching percentage of 80.55% and controls showed a mean matching percentage of 91.73%. All the differences between the study groups and control groups were found to be highly statistically significant ($P \leq .0001$). Additionally, the 3D color map provided by the StS analysis confirmed that the areas expressing the greatest mismatch were mainly localized at the posterior and superior glenoid fossa and articular eminence (Figure 3).

DISCUSSION

The current research evaluated the long-term effects of untreated PUXB on the glenoid fossa and articular eminence shape by analyzing CBCT images of adult subjects with 3D technology to verify any structural asymmetry of the glenoid fossa and articular eminence between the crossbite side and noncrossbite side. The analysis of a CBCT-derived 3D model using StS helped to elucidate if PUXB in adult patients was associated with glenoid fossa and articular eminence asymmetry between the two sides. In fact, StS, a reverse engineering technique, can quantify and finely evaluate, on a colorimetric 3D map, shape differences between superimposed 3D anatomical models, such as the glenoid fossa and articular eminence in the current research. The color map of the overlapped structures derived from StS analysis evaluated and precisely located the asymmetrical areas on the inner surface of the glenoid fossa clearly.

The results corroborated the previous belief[11] and provided new evidence of glenoid fossa and articular eminence adaptive remodeling changes in the TMJ complex[15] in untreated PUXB patients. A higher percentage of glenoid fossa and articular eminence asymmetry was found while comparing the crossbite and noncrossbite sides of PUXB patients compared to the control sample, with mean percentage differences greater than 11 for each level of tolerance.

Although the current data could not be compared to previous findings as no earlier study had investigated the glenoid fossa and articular eminence shapes in detail, nor had 3D technology been used to evaluate TMJ morphology in PUXB patients, they seem to scientifically validate a point of view already hypothesized in the literature. O'Byrn et al.[11] described mandibular positional asymmetry that appeared to be rotated compared to the cranial floor in adult PUXB patients and no differences in the position of the condyle in the fossa. So, they speculated TMJ remodeling as a consequence of unilateral posterior crossbite due to a process of adaptive repositioning[15] of the glenoid fossa between the affected and non-affected sides. Also, an anterior/inferior distraction and medial position of the condyle of the noncrossbite side and a posterior/superior (compression) and lateral position on the crossbite side have been described.[15]

However, no significant differences in condyle position within the glenoid fossa have been reported,[21] nor was there a noticeable mandibular functional shift in untreated adult patients with PUXB.[11] These findings further corroborate the adaptive nature of the glenoid fossa even in PUXB patients, which is known to occur after changes in the occlusion and positioning of the mandible.

Additionally, Pirttiniemi et al.[9] found that PUXB patients have different inclinations of the articular eminence on the crossbite and noncrossbite sides. This was in line with previous data, which demonstrated that deep fossa and eminence slopes undergo continuous morphological alteration throughout adult life and these alterations are probably mediated by dental function and contrasting patterns of tooth use.[22]

The results of the current study demonstrated that the anatomical areas with the highest mismatch (noncorrespondence of shape, ie, asymmetry) were located on the lateral posterior and medial-anterior walls of the glenoid fossa and articular eminence region. In light of these results, it can be assumed that, in adult PUXB patients, a difference in masticatory functional demands[22] and the persistence of asymmetrically positioned condyles in the glenoid fossa, elicited a process of adaptive remodeling of the inner surface of the glenoid fossa, especially in those areas subject to compression and distraction of the mandibular condyles. Hence, this resulted in the different shape of the glenoid fossa itself. The persistence of compression and traction areas on a bone structure brought about active remodeling of the bone due to progressive secondary osteogenic activity.

The findings explained why the location of both condyle heads (crossbite and noncrossbite sides) within the glenoid fossa have been reported as similar and not deviating from normal.[6,14,21] Thus, the original lateral displacement of the mandible must have been compensated with TMJ complex adaptive remodeling of the condyles, glenoid fossae, or a combination of these factors.[6]

This condition raises the question of PUXB correction in adult patients by orthodontic means alone, which might lead to a sudden change in the function of the mandibular condyles. That this fairly sudden change in condyle position might persist beyond adaptive capabilities and lead to discomfort and pain should be taken in account.[11]

CONCLUSIONS

- Posterior unilateral crossbite patients show greater degrees of mismatch between the two sides when analyzing the morphological and shape differences of the glenoid fossa and articular eminence compared to a control group of nonaffected subjects.
- The asymmetry in posterior unilateral crossbite patients is mainly located at the articular eminence and lateral-posterior wall of the glenoid fossa, as revealed by the StS matching technique. The null hypothesis was rejected.

ACKNOWLEDGMENTS

This study was funded by the University of Catania. Piano per la Ricerca 2016-2018 number: 79722042107.

REFERENCES

1. Bjoerk A, Krebs A, Solow B. A Method for epidemiological registration of malocclusion. *Acta Odontol Scand*. 1964;22: 27–41.
2. da Silva Filho OG, Santamaria M, Jr., Capelozza Filho L. Epidemiology of posterior crossbite in the primary dentition. *J Clin Pediatr Dent*. 2007;32:73–78.
3. Day AJ, Foster TD. An investigation into the prevalence of molar crossbite and some associated aetiological conditions. *Dent Pract Dent Rec*. 1971;21:402–410.
4. Gungor K, Taner L, Kaygisiz E. Prevalence of posterior crossbite for orthodontic treatment timing. *J Clin Pediatr Dent*. 2016;40:422–424.
5. Shalish M, Gal A, Brin I, Zini A, Ben-Bassat Y. Prevalence of dental features that indicate a need for early orthodontic treatment. *Eur J Orthod*. 2013;35:454–459.
6. Nerder PH, Bakke M, Solow B. The functional shift of the mandible in unilateral posterior crossbite and the adaptation of the temporomandibular joints: a pilot study. *Eur J Orthod*. 1999;21:155–166.
7. Pinto AS, Buschang PH, Throckmorton GS, Chen P. Morphological and positional asymmetries of young children with functional unilateral posterior crossbite. *Am J Orthod Dentofacial Orthop*. 2001;120:513–520.
8. Kilic N, Kiki A, Oktay H. Condylar asymmetry in unilateral posterior crossbite patients. *Am J Orthod Dentofacial Orthop*. 2008;133:382–387.
9. Pirttiniemi P, Kantomaa T, Lahtela P. Relationship between craniofacial and condyle path asymmetry in unilateral crossbite patients. *Eur J Orthod*. 1990;12:408–413.
10. Pirttiniemi P, Raustia A, Kantomaa T, Pyhtinen J. Relationships of bicondylar position to occlusal asymmetry. *Eur J Orthod*. 1991;13:441–445.
11. O'Byrn BL, Sadowsky C, Schneider B, BeGole EA. An evaluation of mandibular asymmetry in adults with unilateral posterior crossbite. *Am J Orthod Dentofacial Orthop*. 1995; 107:394–400.
12. Lam PH, Sadowsky C, Omerza F. Mandibular asymmetry and condylar position in children with unilateral posterior crossbite. *Am J Orthod Dentofacial Orthop*. 1999;115:569–575.
13. Kecik D, Kocadereli I, Saatci I. Evaluation of the treatment changes of functional posterior crossbite in the mixed dentition. *Am J Orthod Dentofacial Orthop*. 2007;131:202–215.
14. Langberg BJ, Arai K, Miner RM. Transverse skeletal and dental asymmetry in adults with unilateral lingual posterior

crossbite. *Am J Orthod Dentofacial Orthop*. 2005;127:6–15; discussion 15–16.
15. Talapaneni AK, Nuvvula S. The association between posterior unilateral crossbite and craniomandibular asymmetry: a systematic review. *J Orthod*. 2012;39:279–291.
16. Leonardi R, Muraglie S, Crimi S, Pirroni M, Musumeci G, Perrotta R. Morphology of palatally displaced canines and adjacent teeth, a 3-D evaluation from cone-beam computed tomographic images. *BMC Oral Health*. 2018;18:156.
17. Cordasco G, Portelli M, Militi A, et al. Low-dose protocol of the spiral CT in orthodontics: comparative evaluation of entrance skin dose with traditional X-ray techniques. *Prog Orthod*. 2013;14:24.
18. Shaheen E, Khalil W, Ezeldeen M, et al. Accuracy of segmentation of tooth structures using 3 different CBCT machines. *Oral Surg Oral Med Oral Pathol Oral Radiol*. 2017;123:123–128.
19. Leonardi R, Muraglie S, Rugieri M, Barbato E. Three-dimensional evaluation on digital casts of morphologic maxillary teeth symmetry, in patients with unilateral palatally displaced canines. *Am J Orthod Dentofacial Orthop*. 2019; 155:339–346.
20. Veli I, Uysal T, Ozer T, Ucar FI, Eruz M. Mandibular asymmetry in unilateral and bilateral posterior crossbite patients using cone-beam computed tomography. *Angle Orthod*. 2011;81:966–974.
21. Leonardi R, Caltabiano M, Cavallini C, et al. Condyle fossa relationship associated with functional posterior crossbite, before and after rapid maxillary expansion. *Angle Orthod*. 2012;82:1040–1046.
22. Hinton RJ. Changes in articular eminence morphology with dental function. *Am J Phys Anthropol*. 1981;54:439–455.